Bull. Mater. Sci., Vol. 34, No. 3, June 2011, pp. 543–549. © Indian Academy of Sciences.

Visible light photocatalytic properties of novel molybdenum treated carbon nanotube/titania composites

FENG-JUN ZHANG[†] and WON-CHUN OH[*]
School of Materials and Chemical Engineering, Anhui University of Architecture, Anhui Hefei 230022, P. R. China
[†]Department of Advanced Materials & Engineering, Hanseo University, Seosan-si, Chungnam-do 356-706, Korea

MS received 17 August 2010; revised 21 October 2010

Abstract. **Two types of molybdenum–carbon nanotubes and molybdenum treated carbon nanotubes/titania composites were prepared using a sol–gel method. These composites were characterized comprehensively by the Brauer–Emett–Teller (BET) surface area, scanning electron microscopy (SEM), energy dispersive X-ray (EDX) analysis, X-ray diffraction (XRD), transmission electron microscopy (TEM) and UV-vis absorption spectroscopy. It was found that the photocatalytic degradation of a methylene blue solution could be attributed to the combined effects caused by the photo-degradation of titania, the electron assistance of carbon nanotube network, and the enhancement of molybdenum. The proposed redox mechanism of the photodegradation of methylene blue on Mo-CNT/TiO_2 composites is suggested.**

Keywords. **Molybdenum; carbon nanotube; titania; photocatalytic; visible light.**

1. Introduction

TiO_2 has attracted considerable interest as a photo catalyst for various degradation reactions of organic contaminants due to its stability, inexpensive and low biological toxicity (Bessekhouad *et al* 2003; Jung *et al* 2004; Kozlova *et al* 2004). However, the wide technological use of TiO_2 is impaired by its large bandgap (3·2 eV), which requires UV irradiation. Therefore, for practical applications, attempts have been made to support TiO_2 nanoparticles on porous adsorbent materials and to extend the light absorption of the photocatalysts to the visible region (Yoneyama and Torimoto 2000; Bhattacharyya *et al* 2004; Carp *et al* 2004; Hamal and Klabunde 2007; Neren Ökte and Özge 2008). Moreover, several researchers have already attempted to reduce the bandgap energy of TiO_2 through doping with transition metal ions (Di Paola *et al* 2002; Devi *et al* 2009).

Recently, carbon supported catalysts have attracted increasing attention (Farag *et al* 1999; Li *et al* 2001; Fu *et al* 2004; Oh *et al* 2007; Yang *et al* 2007; Oh and Chen 2008; Zhang *et al* 2008, 2009). Carbon nanotubes (CNTs) are a type of novel carbon material with unique mechanical and electronic properties (Dai *et al* 1996; Zhang *et al* 1999), which can be regarded as hollow graphite fibre with a perfect structure, such as seamless tube-like graphitic walls consisting of sp^2 carbon–carbon atoms, nano-sized hollow channels, excellent electron-transporting capability as well as convertible surface properties that can be modified easily. Overall, these properties make CNTs good candidates as catalyst supports.

Doping is also a promising approach for reducing the absorption threshold of TiO_2 and extending its optical absorption range from the ultraviolet to visible region (Asahi *et al* 2001). Therefore, a large number of studies focusing on doping of TiO_2 with metal or nonmetal elements have been reported over the past decade and demonstrated obvious visible-light activity (Thompson and Yates 2006; Chen and Mao 2007). Choi *et al* (1994) examined TiO_2 doped with 21 different transition metal ions and reported a significant increase in the photo-reactivity of TiO_2 samples for both chloroform oxidation and reduction when Fe^{3+}, Mo^{5+}, Ru^{3+}, Os^{3+}, Re^{5+}, V^{4+} and Rh^{3+} were used at 0·1–0·5%. Molybdenum appears to be one of these potentially interesting additives because it is inexpensive and largely available. However, the partially occupied impurity bands can act as recombination centres where photoinduced charge carriers recombine, resulting in a decrease in charge carrier quantity and photocatalytic activity in some single-doped TiO_2.

Although Mo-doped TiO_2 and CNT-supported TiO_2 were reported to exhibit enhanced *vis*-photocatalytic activity compared with pure TiO_2 (Choi *et al* 1994; Oh and Chen 2008; Devi *et al* 2009), there are a few reports on Mo-treated CNT as supported materials for TiO_2 photocatalyst. In this study, Mo–CNT/TiO_2 composites were synthesized using a sol–gel method. The mechanisms of enhanced visible-light activity and photocatalytic performance in Mo–CNT/TiO_2 are discussed.

[*]Author for correspondence (wc_oh@hanseo.ac.kr; zhang-fengjun@hotmail.com)

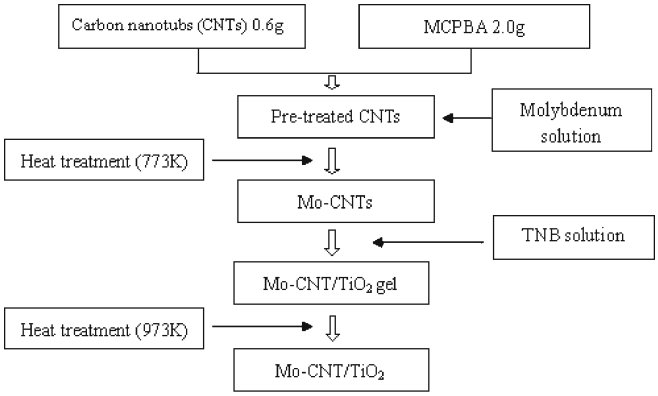

Figure 1. Flow chart of fabrication of Mo–CNT/TiO_2 composites.

2. Experimental

2.1 *Materials*

Carbon nanotubes (CNTs) were selected as the support material. The CNTs (multiwall nanotubes, diameter: ∼20 nm, length: ∼5 μm) were supplied by Carbon Nano-Material Technology Co., Ltd, Korea and used as received. TNB (Ti$(OC_4H_7)_4$) as a titanium source for the preparation of the composites was purchased from Acros Organics, New Jersey, USA. *m*-chloroperbenzoic acid (MCPBA, Acros Organics, New Jersey, USA) was used as an oxidized reagent for oxidization of CNT surface. Analytical grade methylene blue was purchased from Duksan Pure Chemical Co., Ltd, Korea. Ammonium molybdate was obtained from Samchun Pure Chemical Co., Ltd, Korea. The reagent-grade solvents, benzene and ethyl alcohol, were acquired from Duksan Pure Chemical Co. and Daejung Chemical Co., Korea and used as received.

2.2 *Preparation of Mo–CNT composites*

MCPBA (2·0 g) as an oxidizing agent was dissolved in 60 mL benzene. CNTs (0·6 g) were added to the oxidizing agent, heated under reflux for 6 h, filtered and dried. The oxidized CNTs were added to a solution containing ammonium molybdate at various concentrations, and the solutions were then homogenized under reflux at 343 K for 5 h using a magnetic stirrer. After heat treatment at 773 K for 1 h, the Mo treated CNT composites were obtained.

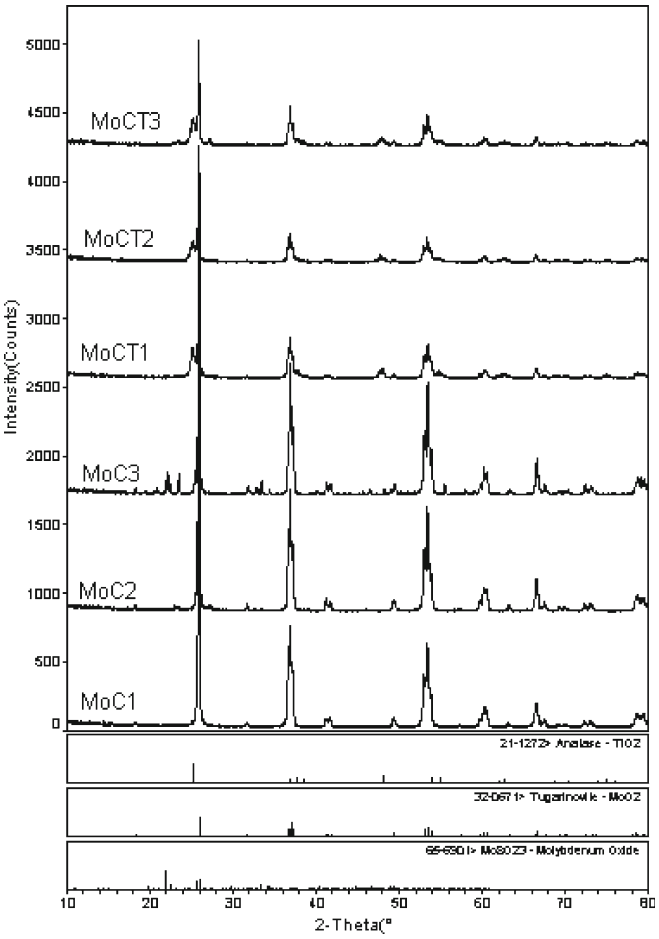

Figure 2. XRD patterns of Mo–CNT/TiO_2 composites.

2.3 *Preparation of Mo–CNT/TiO_2 composites*

The Mo treated CNT composites were placed into the TNB and benzene at a volume ratio of 4:16. The solutions were then homogenized under reflux at 343 K for 5 h. After stirring, the solutions transformed to Mo–CNT/TiO_2 gels. The gels were heated at 973 K for 1 h. After cooling, the Mo–CNT/TiO_2 composites were produced. Figure 1 and table 1

Table 1. Nomenclatures and surface areas of Mo–CNT/TiO_2 composites.

Preparation method	Nomenclatures	S_{BET} (m^2/g)
0·6 g CNT+ ammonium molybdate (0·01M)	MoC1	181
0·6 g CNT+ ammonium molybdate (0·02M)	MoC2	172
0·6 g CNT+ ammonium molybdate (0·03M)	MoC3	165
0·6 g CNT+ ammonium molybdate (0·01M)+TNB 4 mL	MoCT1	106
0·6 g CNT+ ammonium molybdate (0·02M)+TNB 4 mL	MoCT2	101
0·6 g CNT+ ammonium molybdate (0·03M)+TNB 4 mL	MoCT3	94

show the preparation conditions and nomenclatures of the samples.

2.4 *Characterization of the Mo–CNT/TiO_2 composites*

X-ray diffraction (XRD) was used for crystal phase identification and to estimate the anatase-to-rutile ratio. The XRD patterns were obtained at room temperature with a Shimata XD-D1 (Japan) diffractometer using Cu Kα radiation. Scanning electron microscopy (SEM, JEOL, JSM-5200, Japan) was used to observe the surface state and porous structure of the Mo–CNT/TiO_2 composites. Energy dispersive X-ray (EDX) spectroscopy was used to measure the elemental analysis of Mo–CNT/TiO_2 composites. Transmission electron microscopy (TEM, JEOL, JEM-2010, Japan) at an acceleration voltage of 200 kV was used to examine the size and distribution of molybdenum and titanium deposits on CNT surface. The TEM specimens were prepared by placing a drop of a sample solution onto a carbon grid.

2.5 *Photocatalytic (PC) decolourization of MB*

PC decolourization was performed using Mo–CNT/TiO_2 composites in a 100 mL glass container and the system was then irradiated with visible light (8W, KLD-08L/P/N, Fawoo Technology) placed 100 mm from the solution in dark box. Prior to illumination, the composites were impregnated in the pristine MB solution in the dark for 120 minutes to achieve adsorption/desorption equilibrium. The Mo–CNT/TiO_2 composites were placed in 50 mL of $1{\cdot}0 \times 10^{-5}$ mol/L MB solution. The PC degradation of MB was performed using visible light. The PC activity of Mo–CNT/TiO_2 composites

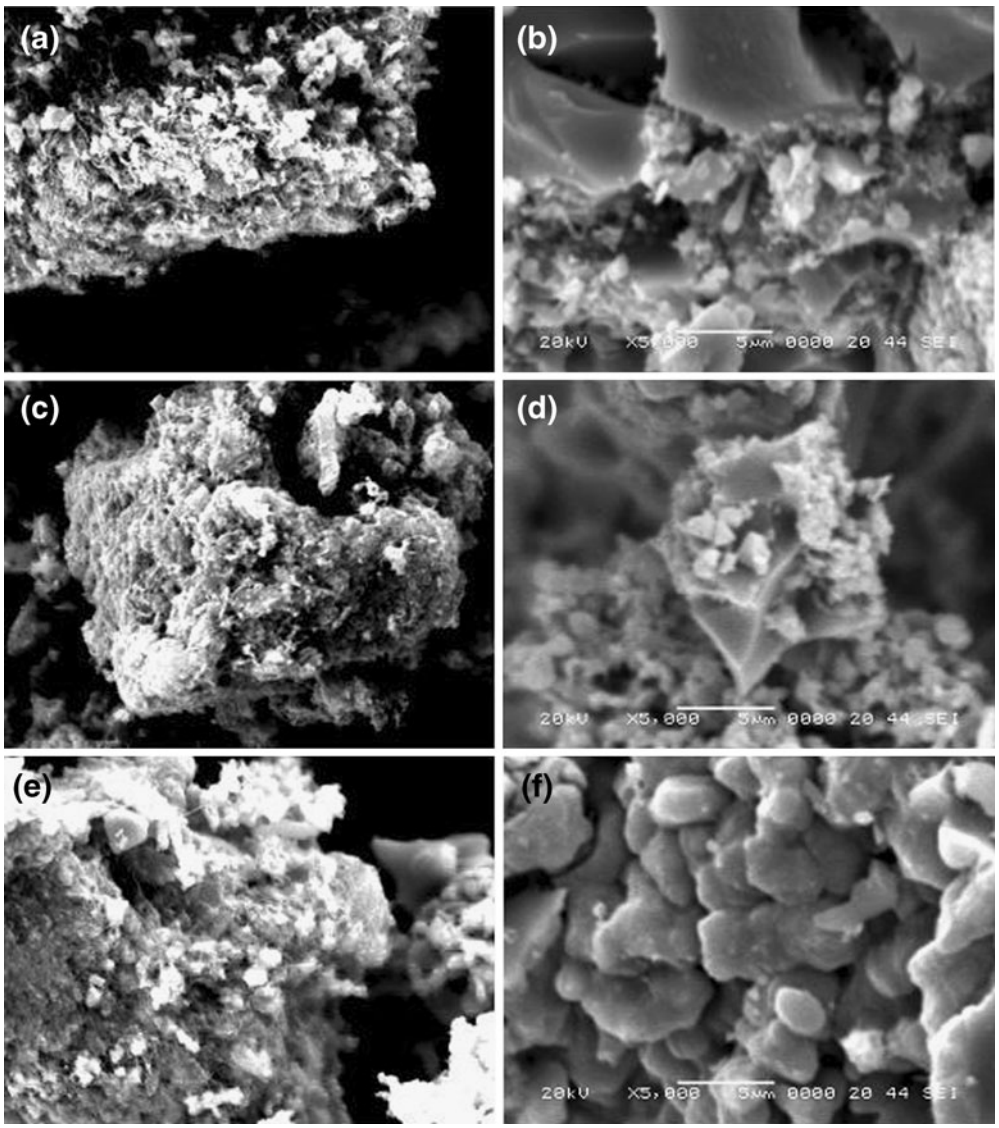

Figure 3. SEM images obtained from powdered Mo–CNT and Mo–CNT/TiO_2 composites. (**a**) MoC1, (**b**) MoCT1, (**c**) MoC2, (**d**) MoCT2, (**e**) MoC3 and (**f**) MoCT3.

was investigated using the rate PC decolourization of the MB solution, which was measured as a function of time. The MB concentration in the solution was determined from the change in absorbance at 660 nm as a function of irradiation time.

3. Results and discussion

3.1 *Structure and morphology of Mo–CNT/ TiO_2 composites*

Table 1 lists the BET surface areas of Mo–CNT and Mo–CNT/TiO_2 composites. The BET surface areas of the molybdenum-treated CNT/TiO_2 composites decreased gradually from 106 to 94 m^2/g with increasing molybdenum concentration but the BET surface areas of non-molybdenum treated CNT/TiO_2 composites also decreased from 181–165 m^2/g. This shows that the BET surface area of the CNT/TiO_2 composite decreases after the formation of TiO_2 particles by TNB treatment. At the same addition of TNB, the intensity of Mo particle aggregation increased with increasing molybdenum concentration. These particles were heavily agglomerated to gather into blocky-shaped particles. These results can be seen clearly from the SEM images obtained from powdered Mo–CNT/TiO_2 composites. The BET surface area of the Mo–CNT/TiO_2 composites decreased after the formation of Mo particles by molybdenum treatment. This suggests that some porosity had developed during heat treatment. The composites are believed to be nano materials with many micropores, which were blocked partially by the formation of Mo particles on the CNT/TiO_2 surface during heat treatment. As expected, the BET surface area decreases due to the blocking of these micropores by surface complexes introduced through the formation of Mo–CNT/TiO_2 composites.

Figure 2 presents XRD results for the catalyst samples. The structure of the molybdenum treated CNT/TiO_2 composites showed an anatase crystal. The crystal structure of titanium dioxide is determined mainly by heat treated temperature. The peaks at 25·3, 37·8, 48·0 and 62·5° 2θ were assigned to the (101), (004), (200) and (204) diffraction planes of anatase, indicating that the developed CNT/TiO_2 composites have an anatase structure when annealed at 973 K.

The XRD patterns of Mo–CNT and Mo–CNT/TiO_2 samples showed (111), (211), (312), (210), (310) and (031) diffraction peaks for the monoclinic MoO_2 phase, which formed during the calcination process. Intense anatase peaks still appeared in the Mo–CNT/TiO_2 samples. Although it is unclear in figure 2, only the MoC3 sample showed MoO_2 and Mo_8O_{23}. Unfortunately, these high angle diffraction peaks are complicated and not easily detected in the figure because of the overlapping diffraction peaks attributed to TiO_2, molybdenum oxides and those of the CNTs support.

The micro-surface structures and morphology of the Mo–CNT/TiO_2 composites were characterized by SEM (figure 3). Figure 3 shows the macroscopic changes in the morphology of the Mo–CNT/TiO_2 composites. As shown in figure 3, the TiO_2 particles were well attached to the surface of the CNT network and the distribution was uniform. Zhang *et al* (2005) reported that a good dispersion of small particles can provide more reactive sites for the reactants than

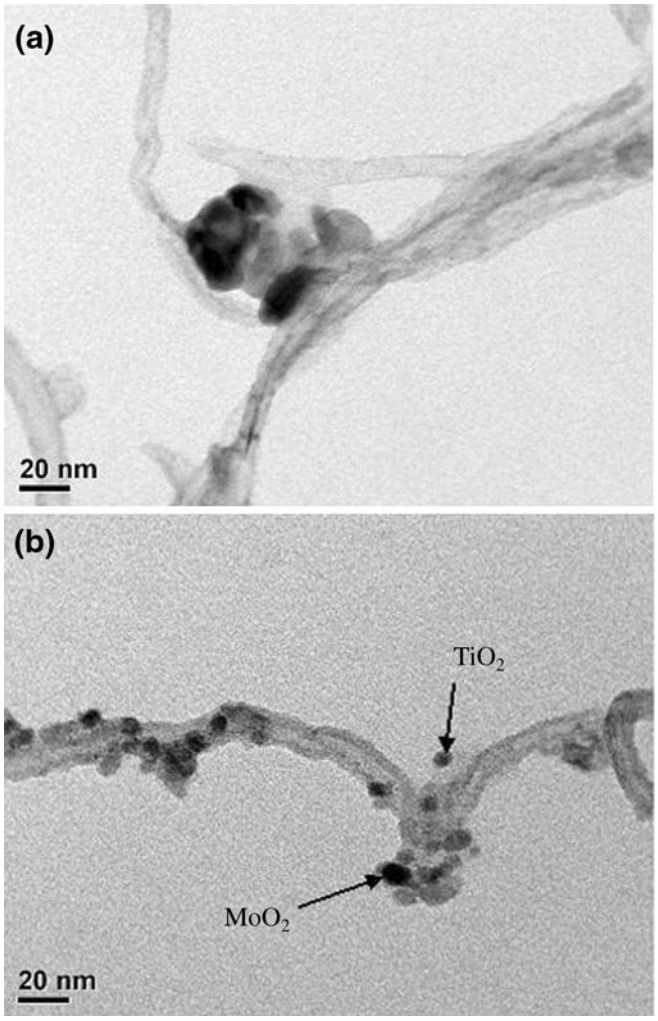

Figure 4. TEM micrographs obtained from powdered Mo–CNT and Mo–CNT/TiO_2 composites. (**a**) MoC3 and (**b**) MoCT3.

Table 2. EDX elemental microanalysis of Mo–CNT/TiO_2 composites.

Samples	Element (wt. %)			
	C	O	Ti	Mo
MoC1	34·2	22·3	0	39·5
MoC2	31·9	20·6	0	47·5
MoC3	29·4	17·6	0	53·0
MoCT1	22·1	40·4	15·1	22·3
MoCT2	23·2	38·8	14·5	23·5
MoCT3	22·2	35·2	13·2	28·4

aggregated particles. At the same time, the conductivity of CNT network can facilitate electron transfer between the adsorbed dye molecules and catalyst substrate (Christensen *et al* 2003), which is beneficial for the enhancement of PC activity of these composites.

Moreover, molybdenum oxide particles were fixed to the surface of the CNT network in small clusters, and the distribution was not uniform. Moreover, for the Mo–CNT samples (figures 3(a), (c), (e)), there was no clear difference in the intensity of aggregation molybdenum oxide particles, but for the Mo–CNT/TiO_2 composites, these particles were heavily agglomerated to form blocky-shaped particles (figures 3(b), (d), (f)), which were more uniform in the MoCT3 sample. These results were confirmed by TEM observations of the Mo–CNT and Mo–CNT/TiO_2 composites. As shown in figure 4, for the Mo–CNT composites, the Mo oxide particles were aggregated on the outer surface of the CNT tubes (figure 4(a)), whereas for the Mo–CNT/TiO_2 composites, the Mo oxide particles attached to the surface of the tubes also caused partial agglomeration to form blocky-shaped particles (figure 4(b)). Moreover, the particle sizes of Mo oxide decrease due to the formation of TiO_2 on the surface of the tubes.

Table 2 lists the results of EDX elemental microanalysis of the Mo–CNT/TiO_2 composites. The content of molybdenum in MoCT1, MoCT2, and MoCT3 was 22·3, 23·5, and 28·4%, respectively. The molybdenum content in the composites increased with increasing molybdenum concentration in the initial solution.

3.2 *PC decolorization of MB*

Figure 5 shows the dark adsorption efficiency of the MoC and MoCT composites for MB degradation. After adsorption in the dark for 2 h, all the samples reached adsorption–desorption equilibrium. The concentration of MB in solution was decreased by only 49·9–72·6% using MoC samples. However, the MoCT samples decreased the concentrations of the MB solution by 36·9–46·0%. For the MoCT samples, the BET surface areas decreased with increasing molybdenum concentration. The results of adsorption are consistent with the BET surface areas.

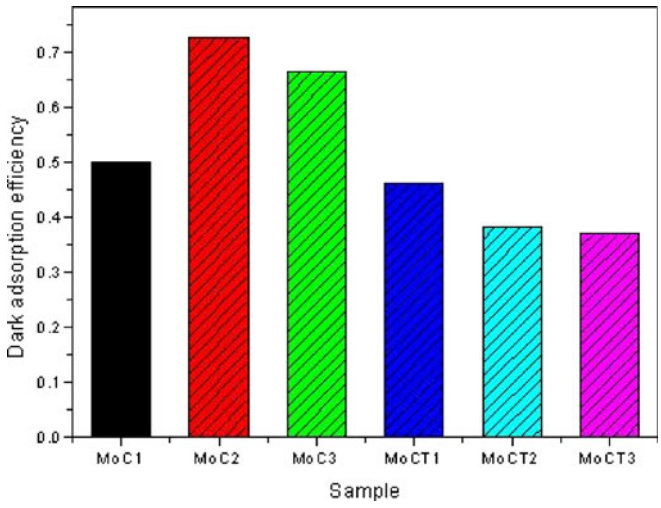

Figure 5. Dark adsorption efficiency of MoC and MoCT composites for MB degradation.

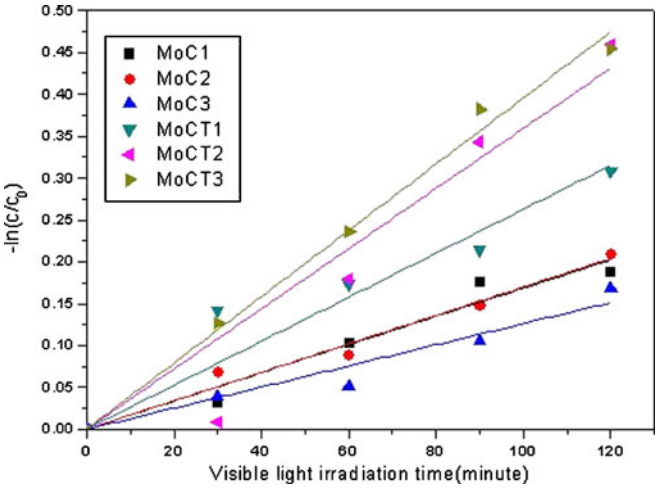

Figure 6. Apparent first-order linear transform –ln(c/c_0) against irradiation time of MB degradation kinetic plots for Mo–C and Mo–CT composites.

Figure 6 shows PC degradation rate of MB for different MoC and MoCT composites under visible light irradiation. The PC effects of the Mo–CNT/TiO_2 composites were superior to that of Mo–CNT at an irradiation time of 120 min. Moreover, for the Mo treated CNT/TiO_2 series, the PC degradation efficiency of the sample MoCT3 was higher than that of the other samples at an irradiation time of 120 min. The catalytic activity of Mo particles for this reaction is dependent on a range of factors, which involves the size and dispersion of the particles, supporting materials and their surface conditions. In the case of MoCT1 and MoCT2, the Mo particles were heavily agglomerated to gather into blocky-shaped particles (figures 3(b) and (f)), which leads to a significant decrease in activity. The PC activity increased with increasing Mo content over a certain range. At the same time, the

Table 3. Kinetic constants of MB degradation.

Photocatalyst	Kinetic constants (k, min^{-1})	Correlation coefficient (R^2)
MoC1	0·00169	0·9818
MoC2	0·0017	0·9914
MoC3	0·00126	0·9737
MoCT1	0·00263	0·9685
MoCT2	0·00359	0·9571
MoCT3	0·00396	0·9965

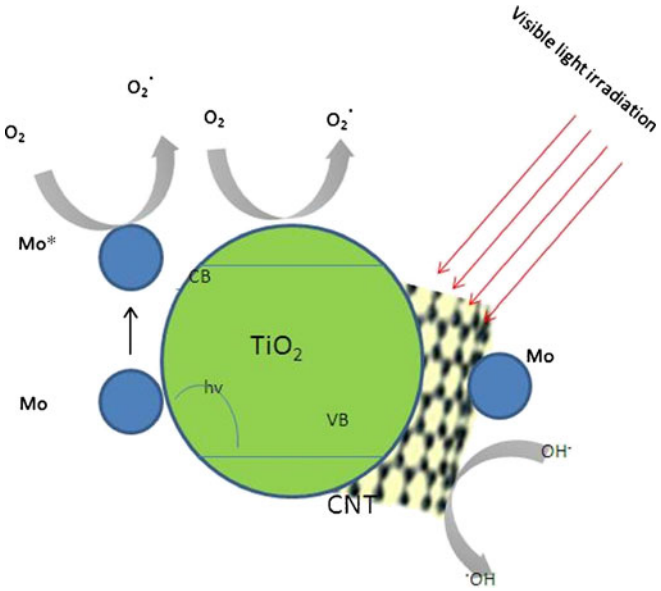

Figure 7. Proposed redox mechanism of Mo–CNT/TiO_2 composites under visible-light irradiation.

morphology of Mo in the Mo–CNT/TiO_2 composites is an important factor.

3.3 *Proposed redox mechanism of Mo–CNT/TiO_2*

Table 3 lists the observed kinetic constants. The first-order kinetics constant increased with increasing Mo addition in the Mo–CNT and Mo–CNT/TiO_2 composites, suggesting that the addition of Mo enhanced the photoactivity. Based on the relevant band positions of Mo and TiO_2, the Mo clusters at lower concentrations acted as a separation centre. The photogenerated electrons were transferred from the TiO_2 conduction band to the Mo conduction band, and holes accumulated in the TiO_2 valence band. Therefore, the photogenerated electrons and holes were separated efficiently. The observed kinetics constants of Mo–CNT were 0·00169 min^{-1} (R^2 = 0·9818), 0·0017 min^{-1} (R^2 = 0·9914) and 0·00126 min^{-1} (R^2 = 0·9737), respectively; and Mo–CNT/TiO_2 were 0·00263 min^{-1} (R^2 = 0·9685), 0·00359 min^{-1} (R^2 = 0·9571) and 0·00396 min^{-1} (R^2 = 0·9965), respectively. Therefore, the first-order kinetics constant of Mo–CNT/TiO_2 was ∼1·5–3·1 times higher than that of Mo–CNT at the same addition of Mo solution. In the case of Mo–CNT/TiO_2, the PC reactions were quite versatile because of the multicomponent nature, and the chemical substances destroyed or transformed photocatalytically is almost unlimited.

MoCT1, MoCT2 and MoCT3 have a good PC activity under visible light irradiation. Figure 7 shows the proposed redox mechanism of Mo–CNT/TiO_2 composites under visible-light irradiation. These electrons tend to reduce the Ti (IV) cations to a Ti (III) state; the holes oxidize O_2^- anions. In this process oxygen atoms are ejected, creating oxygen vacancies. Water molecules can then occupy these oxygen vacancies, producing adsorbed OH groups, which tend to produce HO. The PC activity is enhanced because more OH groups can be adsorbed on the surface. On the other hand, the surface of these composites can adsorb contaminated compounds, which tends to convert the hydrophilic surface to a hydrophobic one. Photocatalysis can decompose the organic pollutants on the surface. The realization of a charge-separated electron transfer with photo-responsive function will lead to an achievement of novel photocatalysts. Such electron transfer has been achieved by semiconductors (Matsui *et al* 2009a, b) and may be achieved by a combination of CNTs and nano-sized semiconductors, in which the carbon parts are expected to act as visible light absorption sites and an electron transfer bed, and semiconductors to act as an electron excitation sites, resulting in visible light absorption and electron excitation.

4. Conclusions

This paper reports the synthesis and characterization of Mo–CNT and Mo–CNT/TiO_2 composites. The surface area of the Mo–CNT/TiO_2 composites decreased due to the presence of molybdenum oxide and TiO_2 particles on the surface of the CNTs. XRD revealed anatase in all samples, and confirmed the crystal structure of MoO_2. The degradation of MB indicated that the addition of molybdenum enhanced the photocatalytic activity of the Mo–CNT/TiO_2 composite. Moreover, the MoCT3 has good photocatalytic activity.

Acknowledgement

This work was supported by the Natural Science Project (KJ2010B047), Education Department of Anhui Province in China.

References

Asahi R, Morikawa T, Ohwaki T, Aoki K and Taga Y 2001 *Science* **293** 269

Bessekhouad Y, Robert D and Weber J V 2003 *J. Photochem. Photobiol. A: Chem.* **157** 47

Bhattacharyya A, Kawi S and Ray M B 2004 *Catal. Today* **98** 431

Carp O, Huisman C L and Reller A 2004 *Prog. Solid State Chem.* **32** 33

Chen X and Mao S S 2007 *Chem. Rev.* **107** 2891

Choi W, Termin A and Hoffmann M R 1994 *J. Phys. Chem.* **98** 13669

Christensen P A, Curtis T P, Egerton T A, Kosa S A M and Tinlin J R 2003 *Appl. Catal. B Environ.* **41** 371

Dai H, Hafner J H, Rinzler A G, Colbert D T and Smaller R 1996 *Nature* **384** 147

Devi L G, Kumar S G, Murthy B N and Kottam N 2009 *Catal. Commun.* **10** 794

Di Paola A, Marci G, Palmisano L, Schiavello M, Uosaki K, Ikeda S and Ohtani B 2002 *J. Phys. Chem.* **B106** 637
Farag H, Whitehurst D D, Sakanishi K and Mochida I 1999 *Catal. Today* **50** 9
Fu P F, Luan Y and Dai X G 2004 *J. Mol. Catal. A: Chem.* **221** 81
Hamal D B and Klabunde K J 2007 *J. Colloid Interf. Sci.* **311** 514
Jung K Y, Park S B and Jang H D 2004 *Catal. Commun.* **5** 491
Kozlova A E, Smirniotis P G and Vorontsov A V 2004 *J. Photochem. Photobiol. A: Chem.* **162** 503
Li Z R, Fua Y L, Bao J, Jiang M, Hu T D, Liu T and Xie Y N 2001 *Appl. Catal. A Gen.* **220** 21
Matsui H, Ishiko A, Karuppuchamy S and Yoshihara M 2009a *J. Alloy Comp.* **473** L33
Matsui H, Nagano S, Karuppucham S and Yoshihara M 2009b *Curr. Appl. Phys.* **9** 561
Neren Ökte A and Özge Y 2008 *Appl. Catal. B: Environ.* **85** 92
Oh W C and Chen M L 2008 *Bull. Korean Chem. Soc.* **29** 159
Oh W C, Jung A R and Ko W B 2007 *J. Ind. Eng. Chem.* **13** 1208
Thompson T L and Yates J T 2006 *Chem. Rev.* **106** 4428
Yang S, Zhu W, Li X, Wang J and Zhou Y 2007 *Catal. Commun.* **8** 2059
Yoneyama H and Torimoto T 2000 *Catal. Today* **58** 133
Zhang Y, Zhang H B, Lin G D, Chen P, Zhu Y and Tsai K R 1999 *Appl. Catal. A Gen.* **187** 213
Zhang X W, Zhou M H and Lei L C 2005 *Carbon* **43** 1700
Zhang F J, Chen M L and Oh W C 2008 *Mater. Res. Soc. Korea* **18** 583
Zhang F J, Chen M L and Oh W C 2009 *Korean Soc. Environ. Eng.* **14** 32